

# Real-time reliability test for a CPV module based on a power degradation model

J.R. González\*, M. Vázquez, C. Algora and N. Núñez

Instituto de Energía Solar – Universidad Politécnica de Madrid (IES-UPM), Avda. Complutense s/n, Ciudad Universitaria, 28040 Madrid, Spain

## ABSTRACT

Models based on degradation are powerful and useful tools to evaluate the reliability of those devices in which failure happens because of degradation in the performance parameters. This paper presents a procedure for assessing the reliability of concentrator photovoltaic (CPV) modules operating outdoors in real-time conditions. With this model, the main reliability functions are predicted. This model has been applied to a real case with a module composed of GaAs single-junction solar cells and total internal reflection (TIR) optics.

## KEYWORDS

reliability; concentrator systems

## \*Correspondence

J.R. González, Instituto de Energía Solar – Universidad Politécnica de Madrid (IES-UPM), Avda. Complutense s/n, Ciudad Universitaria, 28040 Madrid, Spain.  
E-mail: jrgonzalez@ies-def.upm.es

## 1. INTRODUCTION

Photovoltaic concentration has proven to be an effective means for reducing the costs of photovoltaic electricity since the early 1970s [1]. In recent years, significant advances have been made in the field of III–V high-concentrator solar cells, achieving peak efficiencies of 32.6% at 1000 suns for a double-junction solar cell [2] and 41.6% at 236 suns for a triple-junction solar cell [3].

These satisfactory results have crystallized into the first commercial ventures of concentration photovoltaic systems based on III–V solar cells. Representative companies can be found around the world [[www.solarsystems.com.au](http://www.solarsystems.com.au), [www.solfocus.com](http://www.solfocus.com), [www.isofoton.com](http://www.isofoton.com), [www.concentrix-solar.de](http://www.concentrix-solar.de), [www.daido.co.jp](http://www.daido.co.jp), [www.entechsolar.com](http://www.entechsolar.com), <http://www.power-spar.com>, <http://www.pyronsolar.com>, <http://www.sol3g.com>]. At present, there is a total amount of more than 17 MW of concentrator photovoltaic (CPV) systems installed in the world, from which more than 4 MW are based on III–V solar cells [4].

It is well known that silicon flat modules are reliable systems. Nowadays, manufacturers' warranties usually extend to 25 years of use, and are expected to increase to 30 years in the near future [5]. In order to compete with silicon flat modules, CPV systems must be covered by similarly extensive warranties. Before such extensive

warranties may be issued, however, the reliability of these devices must first be confirmed.

Studies have been carried out in an effort to characterize the degradation and the reliability of III–V concentrator solar cells [6,7]. In view of the similarities between solar cells and light emitting diodes (LEDs), the lifespan of CPV solar cells was predicted to be characterized by a mean time to failure (MTTF) of up to  $10^5$  h [8] (equivalent to 34 years assuming an average of 8 h of operation per day). This prediction has been corroborated by an accelerated aging test in which a functional MTTF persisted longer than 69 years with a 90% unilateral confidence interval [9].

Therefore, the first set of reliability studies on bare III–V concentrator solar cells have already been conducted, but the reliability of the module has not yet been determined. Reliability models [10–13] based on performance degradation parameters are very useful in elements which main failure mechanism is degradation because it is possible to obtain reliability functions in a short time of accelerated tests or real working conditions. A reliability model based on degradation has been proposed for conventional Si modules by the authors in a previous work [14], in which a reliability model for silicon flat modules was presented, obtaining the main reliability functions from field degradation data. In that work, a large population of Si modules working during a long period of time was

considered. Catastrophic random failures were not considered in Ref. [14], and the reliability functions were evaluated considering the whole set of different degradation mechanisms, making no difference between them.

The aim of this work is to present a procedure for assessing the reliability functions of CPV modules operating outdoors in real-time conditions. As it will be shown later, the power evolution and the failure analysis identify, beyond doubt, a degradation process in the optics. Accordingly, the analysis with reliability models based on degradation is justified. Even though this procedure has been applied to a particular case and the reliability of the module was seriously affected by the features of the assembly, this fact does not have any influence in the procedure, and it can be easily generalized to other different CPV technologies where failure is caused by degradation in power.

## 2. EXPERIMENTAL SET-UP

For this test, a module composed of 32 GaAs single-junction solar cells with TIR (total internal reflection) [15] optics was used (see schematic of Figure 1). The module was outdoor-tested for 7 months. This CPV module featured an assembly that allowed independent electrical access to every receiver<sup>a</sup> contained therein. The evolution of each of these receivers was followed independently, avoiding the “hiding effect” in performance degradation that results from a single measurement of a series or parallel configuration in a conventional assembly. The module was mounted on a two-axis sun tracker installed on the flat roof of IES-UPM (see Figure 2).

A data acquisition system was developed to periodically measure  $I-V$  curves of the solar cells. This system consisted of two parallel connected multiplexers with 32 channels that allowed selection of the solar cell for measurement, a data acquisition card, an active load for

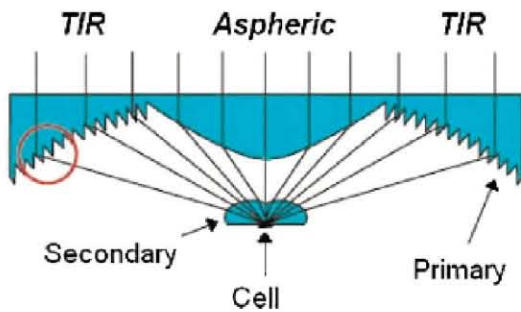


Figure 1. Schematic of total internal reflection (TIR) optics [15].

<sup>a</sup>For the sake of simplicity, a receiver in this work is considered to include: primary and secondary elements of the optics as well as the encapsulated solar cell.



Figure 2. Two-axis sun tracker installed on the flat roof of the Instituto de Energía Solar – Universidad Politécnica de Madrid (IES-UPM).

measuring  $I-V$  curves, a software environment specifically designed for this system, and an uninterruptible power supply. Irradiance and wind speed were obtained from the IES Meteorological Station [<http://helios.ies-def.upm.es/>].

The data acquisition system periodically recorded the following information:

- Illumination  $I-V$  curves of each individual solar cell every 15 min from 10:00 to 17:00 h.
- Dark  $I-V$  curves for each individual solar cell once a day at 02:00 h.
- Direct irradiance and ambient temperature data synchronized with the  $I-V$  curve measurement.

Dark and illumination  $I-V$  curves were recorded to follow the evolution of the solar cells. With every measurement, the temperature and irradiation data were also collected for normalization. The temperature of the modules was measured at the back side. The thermal difference between the back side and the junction of the solar cell was estimated to be 60°C [16].

The illumination  $I-V$  curves were normalized using the equations proposed by the Instituto de Sistemas Fotovoltaicos de Concentración (ISFOC) [[http://www.icmf.es/icmf/ISFOC/PLIEGOCONDICIONES\\_Esp.pdf](http://www.icmf.es/icmf/ISFOC/PLIEGOCONDICIONES_Esp.pdf)]. Based on this method, the points  $(V_i, I_i)$  measured at a cell temperature  $T_{cell}$  with a direct normal irradiance  $B_{med}$ , were converted to new operating conditions characterized by a new cell temperature  $T_{oper}$  and a new irradiance  $B_{oper}$ . The new points are given by  $(V_i + \Delta V_i, I_i(B_{oper}/B_{med}))$ , where  $\Delta V_i$  is defined by

$$\Delta V_i = \frac{0.0257(T_{oper} - T_{cell})}{297} \left[ \ln \frac{I_{L,med} - I_i}{I_{med}} \right] + (E_g - V_{oc,med}) \left( 1 - \frac{T_{oper}}{T_{cell}} \right) \quad (1)$$

where temperatures are given in Kelvin,  $E_g$  is the band gap energy (eV),  $I_{L,med}$  is the short circuit current (A), and  $V_{oc,med}$  is the open circuit voltage (V).

The normalized curves obtained by the method described were used to follow the power output of the solar cells and thus to obtain the main reliability functions.

### 3. CHARACTERIZATION OF FAILURE MECHANISMS

This paper proposes a model for assessing the reliability of a CPV module and estimating the main reliability functions.

We introduce several definitions that are used throughout the following description of the model:

- *Failure*: The termination of the ability of an item to perform a required function (IEC 60050-191) [17].
- *Failure mechanism*: The physical, chemical, or other process that may lead to failure (IEC 60050-191).
- *Failure mode*: The effect by which the item is observed to fail.

Failures can be categorized into two groups:

- *Catastrophic*: are those sudden and total failures from which recovery is impossible. These failures occur in a very short period of time, with limited or no warning. In this case, the reliability assessment is based on a time-to-failure distribution fitted by time-to-failure data.
- *Degradation*: are those soft and gradual failures revealed by means of degradation in the performance of the device. Signals that warn the occurrence of failure appear if the device is properly monitored. Operability occurs when the parameter characterizing the device performance remains within a given margin. Otherwise, the device is assumed to have failed.

Often, there can be more than one failure mode for a type of device. Because a non-repairable device can only fail once, however, only one failure mode is responsible for causing the failure of a single device.

All failures registered in the tests presented here resulted from the degradation of the power output. This failure mode could be produced by different failure mechanisms and is analyzed in the following sections.

The power output is assumed to suffer degradation over time. The  $i$ th failure mechanism affected the degradation of the power output in the following way:

$$P(t) = P_0 \gamma_i(t), \quad (2)$$

where  $\gamma_i(t)$  decreases with time,  $\gamma_i(0) = 1$  and  $\gamma_i(\infty) = 0$ .

Considering  $n$  independent degradation failure mechanisms, the power output will degrade as according to

$$P(t) = P_0 \prod_{i=1}^n \gamma_i(t), \quad (3)$$

where  $P(0) = P_0$  and  $P(\infty) = 0$ .

For the sake of simplicity, the degradation of the power output in CPV modules was assumed to arise from the contributions of two failure mechanisms:

- *Optical degradation mechanism* ( $\gamma_{opt}$ ): produced by degradation in the optical system, due to loss of light transmission through the optics, misalignment of the optical elements, or degradation of the AR coatings on the solar cells.
- *Electrical degradation mechanism* ( $\gamma_{elec}$ ): produced by degradation of the solar cell or contacts (wire-bonding connections).

Therefore, for every receiver of the module, the time evolution of the power output is described by means of the following expression:

$$P(t) = P_0 \gamma_{opt}(t) \gamma_{elec}(t) \quad (4)$$

The goal of this model is to assess the influence of each module component on the degradation of overall module power generation.

The module receivers were electrically isolated from each other, and independent electrical access was provided to each. In this way, the reliability study independently studied each receiver. Overall reliability depends on whether the receiver configuration is set up in series or parallel, as will be discussed in Section 5. In a series configuration, if any single receiver fails, the entire association could fail<sup>b</sup> although this will depend on whether the cell fails open or shorted. In a parallel configuration, the association of receivers will continue to operate until the number of failed receivers reduces the delivered power below a predefined value.<sup>c</sup>

### 4. MODELING RELIABILITY BASED ON DEGRADATION

Reliability is the ability of a system or component to perform its required functions under stated conditions for a specified period of time. Reliability of a device or system is, therefore, evaluated by precisely defining the required function performance criteria.

In a CPV module, the required function is related to the output power delivered. The output power required for module performance is defined with respect to the initial value. If, at a given time, the power produced by a solar cell is higher than a predefined value ( $P_{limit}$ ), then the module is considered to work properly. If the power produced by a solar cell is lower than  $P_{limit}$ , then the module is considered to have failed.

In this section, a reliability model based on degradation is proposed. This model is intended to be a valuable tool for predicting reliability.

<sup>b</sup>A series system, from the reliability point of view, fails if one of its elements fails.

<sup>c</sup>A parallel system, from the reliability point of view, works if one of the elements works.

Reliability predictions based on degradation are an efficient method for estimating the reliability of highly reliable devices when the observation of failures is rare. Reliability estimates of silicon flat modules have been made by this method, and a complete review can be found in Ref. [14]. With this method, it is possible to obtain analytical expressions for the reliability function, the failure probability density function, the instantaneous failure rate function, and the MTTF. The model allows estimation of reasonable power warranties as well as other statistical parameters.

This model considers the following assumptions:

- Solar receivers are composed of solar cells and their entire optical system. The solar cell includes front and back electrical connections. The optical system consists of primary and secondary elements.
- The illumination  $I-V$  curve for each receiver is periodically measured. This measurement provides information regarding the entire receiver (i.e., optics and solar cell).
- The dark  $I-V$  curve is also periodically registered for every receiver. This measurement provides information regarding only the solar cell.
- The power generated by the receiver is the reference parameter for evaluating degradation. Manufacturers of conventional silicon flat modules also use power output to assess performance.
- The failure of each receiver is defined with respect to its initial power. If, at a given time, the power produced by a receiver is lower than  $P_{\text{limit}}$ , the receiver is considered to have failed.
- For a batch of receivers, the power follows a normal distribution with an average and a standard deviation. Accordingly, the associated power probability density function is

$$p(P, t) = \frac{1}{\sqrt{2\pi}\sigma(t)} \exp\left[-\frac{1}{2}\left(\frac{P(t) - \mu(t)}{\sigma(t)}\right)^2\right], \quad (5)$$

where  $P(t)$  is the power of the receiver,  $\mu(t)$  is its average value, and  $\sigma(t)$  its standard deviation. All values are expressed in  $W_p$ .

- The average power and the standard deviation of the receiver are time-dependent functions. Initially, the power has a nominal value,  $P_0$ , and the standard deviation presents the lowest value, related to the fabrication tolerance of the receivers. The mean power decreases with time and the standard deviation increases, similar to silicon flat modules [14].

In this work,  $\mu(t)$  and  $\sigma(t)$  were obtained experimentally. Thus,  $p(P, t)$  can be determined using Equation (5). Figure 3 shows the normalized probability density functions at several points in time. The power limit is represented by a horizontal line. The following sections will discuss the origin of the exponential time dependence of the mean power.

In terms of statistical reliability analysis, the reliability,  $R(t)$ , is a time-dependent function that gives the probability

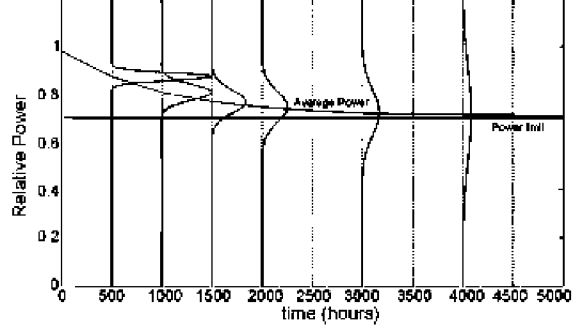


**Figure 3.** Time evolution of the average power and the standard deviation.

of an item operating for a certain period of time without failure. In the case of a batch of receivers, the reliability function gives the probability that, at a given time, the power of a receiver in that batch is higher than some power limit that corresponds to the definition of failure ( $P_{\text{limit}}$ ). According to this definition,  $R(t)$  can be calculated by integrating the power probability density function introduced in Equation (5), as follows:

$$R(t) = \int_{P_{\text{limit}}}^{\infty} p(P, t) dP = 1 - \Phi\left(\frac{P_{\text{limit}} - \mu(t)}{\sigma(t)}\right), \quad (6)$$

where  $\Phi$  is the cumulative probability function for the Gaussian distribution. Using Equation (6), the reliability of a photovoltaic module can be evaluated at any time as a function of the parameters  $P_{\text{limit}}$ ,  $\mu(t)$ , and  $\sigma(t)$ .

The probability density function associated with the random variable time to failure is called failure probability density function,  $f(t)$ , and is obtained by means of the following expression:

$$f(t) = -\frac{dR(t)}{dt}. \quad (7)$$

The instantaneous failure rate determines the number of failing receivers, per unit time, among the surviving ones. The function  $\lambda(t)$  is calculated as the ratio of the failure probability density function to the reliability function:

$$\lambda(t) = \frac{f(t)}{R(t)}. \quad (8)$$

The MTTF can also be calculated by integrating Equation (6):

$$\text{MTTF} = \int_0^{\infty} R(t) dt. \quad (9)$$

## 5. FAILURE ANALYSIS

Figure 4 shows the dark  $I-V$  curves for one of the solar cells assembled in the module. The slight variation among curves plotted in Figure 4 is due to the different



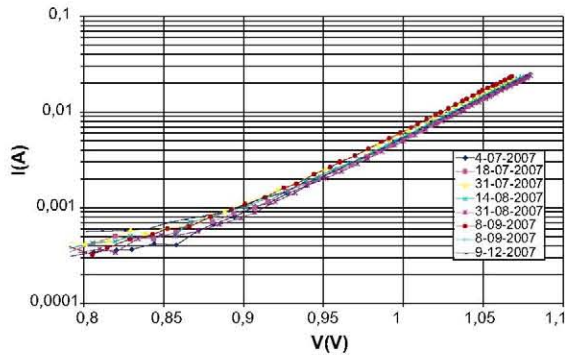


**Figure 4.** Dark  $I$ - $V$  curve evolution for one solar cell. Curves are not corrected for temperature.

temperatures at which cells were registered. Normal operation of the cells produced no change.

To evaluate failure, it is necessary to define failure precisely. In this test, failure of a single receiver was defined as a power loss of 30% or more with respect to the initial value ( $P_{\text{limit}} = 0.7P_0$ ).

After installation of the module on the tracker, only eight receivers were operable. These receivers were tested during 187.5 days. Variations in  $V_{\text{oc}}$  and  $I_{\text{sc}}$  for these receivers are presented in Figure 5. The  $V_{\text{oc}}$  presents only a slight variation at the end of the test. In contrast,  $I_{\text{sc}}$  presents variations of up to 45%.

Failure analysis was carried out by detaching the various module elements after the test. This analysis showed that the reduction in  $I_{\text{sc}}$  was produced by both misalignment and leak of the silicone used for sealing. To support this assertion, additional measurements were performed in two cases:

- (a) Due to poor sealing of the optics, silicone invaded the outer rings of the TIR lens, as can be seen in Figure 6. The illumination  $I$ - $V$  curves for some of these receivers

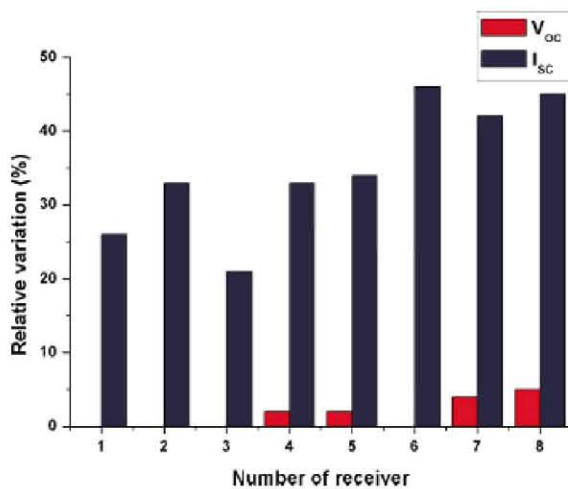


**Figure 5.**  $V_{\text{oc}}$  and  $I_{\text{sc}}$  decrease for the eight working receivers.

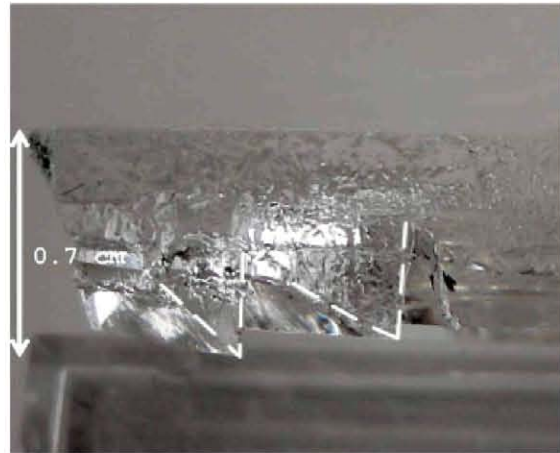


**Figure 6.** Lateral view of the primary element of the optics.

were measured under a solar simulator, firstly with the TIR lenses contaminated by leaked silicone, and secondly, with clean lenses. Variations in  $I_{\text{sc}}$  of up to 20% were found in both measurements, as can be seen in Figure 7.

- (b) Independent electrical access to every receiver necessitated manual assembly of the modules. Manual assembly introduced misalignment in the optics because the mechanical stability of the module was affected by both the electrical isolation of each receiver and the high number of wires needed to contact each one. Two illumination  $I$ - $V$  curves were measured for a selection of receivers during module detachment: with the receiver in the relaxed position and with forced misalignment of about  $2^\circ$  (this angle represents the deviation of the optics' housing with respect to the external glass) as can be seen in Figure 8. Variations of up to 13% in the  $I_{\text{sc}}$  were found, as can be seen in Figure 9.

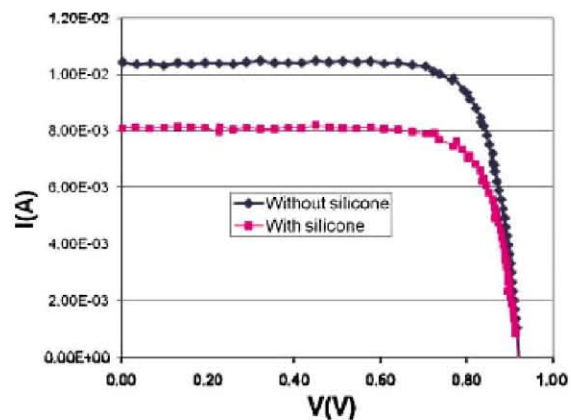


**Figure 7.** Illumination  $I$ - $V$  curves for a receiver with a primary lens containing the remains of leaked silicone and a clean primary lens.

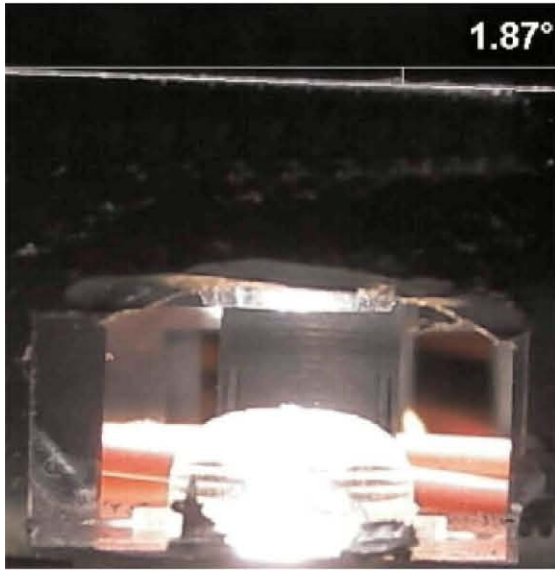


**Figure 8.** Cross-section of the receiver after detachment, with a torqued inclination of  $1.87^\circ$  (this angle represents the deviation of the optics' housing with respect to the external glass).

Therefore, failure analysis revealed that failure in the receivers is related to both optical alignment and silicone leak. No yellowing has been observed. The degradation of the solar cells occurs on a longer timescale than the time frame of this set of experiments. Therefore, to reveal the failure modes of the solar cell, accelerated aging tests were carried out [9]. The tests carried out in Ref. [9] yielded an MTTF of more than 60 years, confirming that the solar cell

was not responsible for failure. Consequently, the value of  $\gamma_{elec}$  is considered to be unity during this test. This implies no influence of the solar cell on the degradation of the receiver performance.

A thorough assessment of a module's reliability must include the influence of the connections between receivers. Two extreme situations may be considered:

1. All receivers connected in parallel. The voltage produced by the module association is the voltage of the receiver with the lowest value. Because the values of  $V_{oc}$  were almost constant during the test, the power loss due to the decrease in the voltage was expected to be low, because all cells worked at a similar value. Loss in power would be caused by a decrease in the sum of the currents due to degradation of the optical system. The reliability of the module would be higher than the reliability of the worst cell and slightly lower than the average of the receivers.
2. All receivers connected in series. The current would be that of the receiver with the lowest value. The best receiver would be working at the current of the receiver with the worst value. The voltage would be the sum of the values of the receivers, but these voltages would be reduced by the limited current, because the current limit changes the working point. Reliability would be lower than that of the worst receiver.

In this test, only defects that affect the optical system were observed. With this consideration, increased reliability would be best achieved by parallel association rather than series.

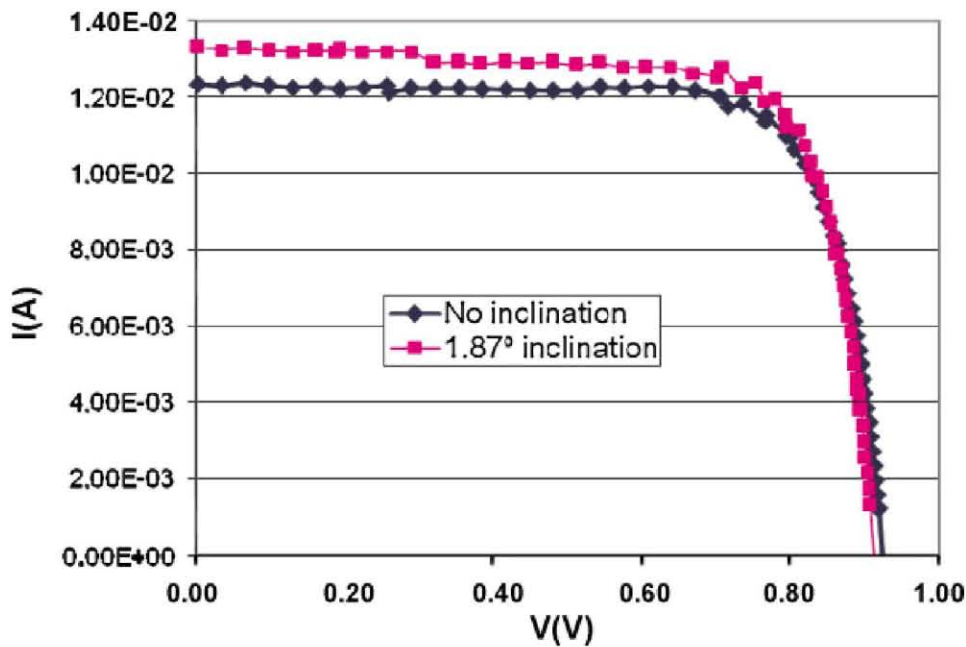


**Figure 9.** Illumination  $I$ - $V$  curves for a receiver in a relaxed position or with a torqued inclination of  $1.87^\circ$ .



## 6. CALCULATION OF THE RELIABILITY FUNCTIONS BY THE MODEL BASED ON DEGRADATION

The main reliability functions are determined in this section. To accomplish this, a model consisting of three hypotheses is proposed. This model is based on a previously described model [14] with modifications introduced to improve the description of concentrator modules, considered here.

The following assumptions must be taken into account:

1. The power is the parameter that is used to follow the evolution of the receivers.
2. The power of the receivers is normalized to its initial value. Normalization provides an assessment independent of the initial dispersion. Therefore, the standard deviation is considered to be zero at the beginning.

The following hypotheses form the basis of the statistical model for reliability:

- **Hypothesis 1:** The powers of the receivers at a particular point in time follow a Gaussian (normal) distribution. To verify this hypothesis, the normalized power of the receivers is represented in a normal probability plot for different points in time (see Figure 10). In this representation, a straight line implies that the data follow a normal distribution, as is the case considered here. A mean correlation coefficient of 0.97 ( $\pm 3\%$ ) is obtained for the plots of Figure 10.
- **Hypothesis 2:** The mean power of the receivers decreases exponentially. Therefore, the mean power would be described as

$$\mu(t) = A \exp(-\alpha t) + y_0. \quad (10)$$

The parameters of this equation were fitted using a nonlinear least squares method, with the following results:  $y_0 = 0.71 \pm 0.01$ ,  $A = 0.27 \pm 0.02$ , and

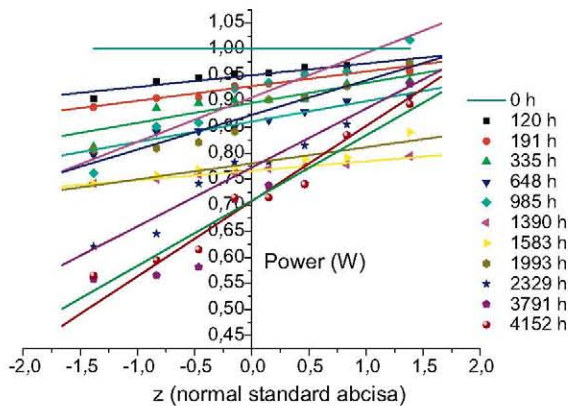


**Figure 10.** Time-dependent normal distribution of power for the receivers.

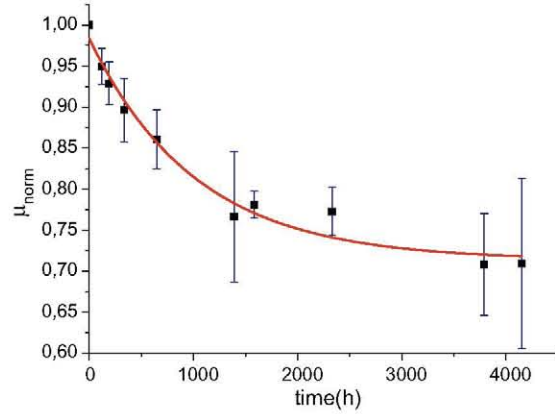


**Figure 11.** Time dependence of the mean power, following a decreasing exponential.

$\alpha = (10 \pm 2) \times 10^{-4} \text{ h}^{-1}$ . Because normalized values were considered,  $y_0$  and  $A$  are dimensionless. The experimental points and the fitting curve are shown in Figure 11. Excellent agreement between data and experiment is characterized by a correlation coefficient of  $R^2 = 0.98$ .

- **Hypothesis 3:** The standard deviation of the normalized mean power increases linearly with time. Therefore, the standard deviation would be described as

$$\sigma(t) = \sigma_0 + Bt, \quad (11)$$

where  $\sigma_0$  is the standard deviation at  $t = 0$ , and  $\sigma_0 = 0$  because all powers were normalized to the initial value. The parameter  $B$  was fit using the least squares method, yielding:  $B = (3.2 \pm 0.3) \times 10^{-5} \text{ h}^{-1}$ . The experimental points and the fitted straight line are presented in Figure 12. The correlation coefficient is 0.90.

Combining the previous hypotheses, which have been shown to be reasonable, and Equation (5), the power

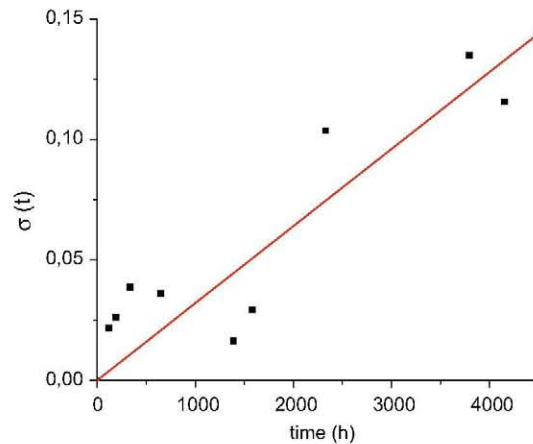


**Figure 12.** Time dependence of the standard deviation of the mean power.

follows the time-dependent probability distribution:

$$p(P) = \frac{1}{\sqrt{2\pi}(\sigma_0 + Bt)} \exp\left[-\frac{1}{2}\left(\frac{P - (A \exp(-\alpha t) + y_0)}{\sigma_0 + Bt}\right)^2\right]. \quad (12)$$

Substitution of the parameters obtained in the previous discussion yields a numerical expression for the previous equation:

$$p(P) = \frac{1}{3.2 \times 10^{-5} \sqrt{2\pi}} \exp\left[-\frac{1}{2}\left(\frac{0.29 - (0.27 \exp(-10^{-3}t))}{3.2 \times 10^{-5}t}\right)^2\right]. \quad (13)$$

The graph of Figure 11 shows that the mean power tends asymptotically to 0.71. This behavior is not typical<sup>d</sup> of degradation processes, but it has been observed in other optoelectronic devices [18]. The physical explanation of this behavior can be found in both the mechanical degradation, causing the optics' misalignment, and the silicone's leak. These circumstances are responsible for an initial fast power loss (within the first 2000 h). However, these mechanisms do not speed up endless; on the contrary they tend to stabilize.

The model described above allows calculation of the main reliability functions. The reliability function can be obtained from the following integral:

$$R(t) = \int_{P_{\text{limit}}}^{\infty} p(P, t) dP. \quad (14)$$

Taking into account the expression of the probability distribution described in (13), the reliability function can be written as

$$R(t) = 1 - \Phi\left(\frac{-0.01 - 0.27 \exp(-10^{-3}t)}{3.2 \times 10^{-5}t}\right), \quad (15)$$

where  $F$  is the cumulative probability function for the normal distribution. The reliability function is plotted in the graph of Figure 13.

The failure probability density function can be obtained by means of Equation (7). This function is plotted in the graph of Figure 14.

The instantaneous failure rate function  $\lambda(t)$  represents the frequency at which devices fail or, in other words, the number of failures per unit time. This function can be calculated using Equation (8). This failure rate function is represented in Figure 15.

The last characteristic reliability parameter that is presented here is the MTTF. This parameter can be obtained by solving the integral of Equation (9). This calculation yields a value for the MTTF of 7080 h (about 1 year). This is an extremely low value when compared with the expected lifetime for a module, 25–30 years.

<sup>d</sup>Typical behavior implies a continuous decrease in the mean power.

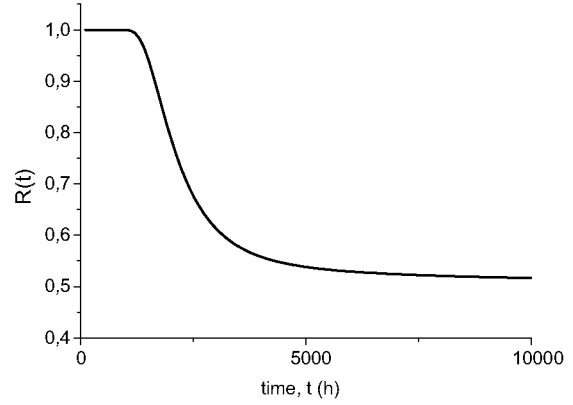


**Figure 13.** Time-dependent reliability function following Equation (15).

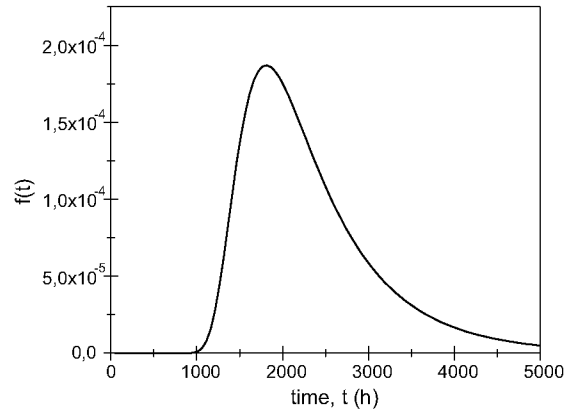


**Figure 14.** Failure probability density function obtained by means of Equation (7).

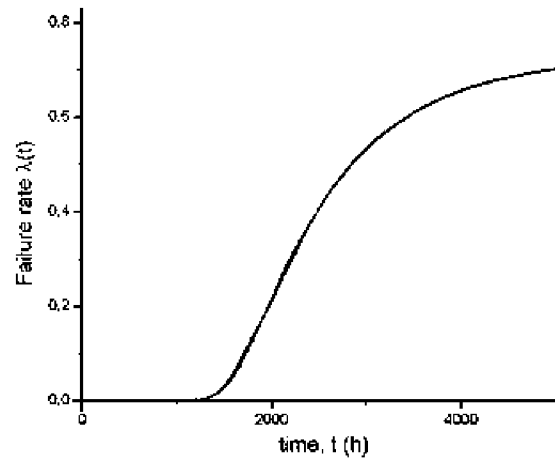


**Figure 15.** Instantaneous failure rate function following Equation (8).



## 7. SUMMARY AND CONCLUSIONS

A statistical model for assessing the reliability of a CPV module based on degradation data was presented in this work. The model was applied to a CPV module manufactured for the purpose of assessing reliability. Independent electrical access was provided to each receiver in the module to evaluate performance over time without the masking effects that a series or parallel connection configuration may introduce.

The main conclusions of this work are:

- A statistical model was proposed to assess the reliability of a photovoltaic module working outdoors in real time.
- The reliability model based on degradation data is based on three hypotheses, which allows the calculation of the main reliability functions.
- The model was applied to a real case: a CPV module with TIR optics and single-junction GaAs solar cells.
- After an initial burn-in period (where failures due to the manipulation of receiver's electric connections were detected) the test failure mechanisms have been only localized to the optics.
- Loss in power output was produced by degradation of the optics (bad sealing and misalignment). This type of evolution is observed in other optoelectronic devices. Optical degradation was evaluated by means of the  $I-V$  curves under illumination and visual inspection of the module. The problems in the optics were assessed by comparison to measurements under a solar simulator.
- The  $I_{sc}$  suffered a strong decrease with time, whereas the variation in  $V_{oc}$  was not significant. For this failure mechanism, the parallel association would be more reliable than the series one.
- Solar cells did not suffer degradation during the test, as can be determined by the analysis of the dark  $I-V$  curves.
- The failure rate of the experimental module increased with time according to a degradation process. The MTTF yielded a value of 7080 h, which is extremely low compared to the expected lifetime of a photovoltaic system ( $\sim 25$  years). The manual assembly of the module may be one reason for such a low value of the MTTF.

This model presents an application of a procedure for evaluating the reliability of CPV modules in real-time testing.

## ACKNOWLEDGEMENTS

The authors would like to thank ISOFOTON, S.A. for supporting this research. The authors would like to thank also Mathieu Baudrit for his kind help with assembling the measurement equipment. This work has been supported by the Spanish Ministerio de Educación y Ciencia with the CONSOLIDER-INGENIO 2010 program by means of the GENESIS FV project (CSD2006-004). The Spanish

Ministerio de Ciencia e Innovación has also contributed with the SIGMASOLES project (PSS-440000-2009-30) and with the project with reference TEC2008-01226 as well as the Comunidad de Madrid under the NUMANCIA II program (S2009/ENE1477).

## REFERENCES

1. Luther J, Luque A, Bett AW, Dimroth F, Lerchenmüller H, Sala G, Algora C. *Concentration photovoltaics for highest efficiencies and cost reduction. 20th European Photovoltaic Solar Energy Conference*, Barcelona, Spain, 2005.
2. Algora C, Rey-Stolle I, García I, Galiana B, Baudrit M, Espinet P, Barrigón E, Datas A, González JR, Bautista J. *A dual junction solar cell with an efficiency of 32.6% at 1000 suns and 31.0% at 3000 suns. 5th International Conference for the Generation of Electricity*, Palm Desert, November 2008.
3. King RR, Boca A, Hong W, Liu X-Q, Bhusari D, Larrabee D, Edmondson KM, Law DC, Fetzer CM, Mesropian S, Karam NH. *Band-gap-engineered architectures for high-efficiency multijunction concentrator solar cells. 24th European Photovoltaic Solar Energy Conference and Exhibition, Hamburg, September 2009.*
4. Rubio F, Banda P. "Concentrated photovoltaics: the path to high efficiency". PVI02-08\_6. Published in PVtech Magazine Fourth Quarter, 2008.
5. Wohlgemuth JH, Cunningham DW, Nguyen AM, Miller J. Long term reliability of PV module. *20th European Photovoltaic Solar Energy Conference, Barcelona, Spain, 2005; 1942-1946.*
6. Araki K. Development of a new 550X concentrator module with 3J cells-performance and reliability. *Proceeding of the 31st IEEE Photovoltaic Specialist Conference*, 2005.
7. Van Riesen S, Bett. AW. Degradation study of III-V solar cells for concentrator applications. *Progress in Photovoltaics: Research and Applications* 2005; **13**: 369-380.
8. Vázquez M, Algora C, Rey-Stolle I, González JR. III-V Concentrator solar cell reliability prediction based on quantitative LED reliability data. *Progress in Photovoltaics: Research and Applications* 2007; **15**(6). 477-491.
9. González JR, Vázquez M, Núñez N, Algora C, Rey-Stolle I, Galiana B. Reliability analysis of temperature step-stress tests on III-V high concentrator solar cells. *Microelectronics Reliability* 2009; **49**: 673-680. 10.1016/j.microrel.2009.04.001.
10. Coit DW, Evans JL, Vogt NT, Thomson JR. A method for correlating field life degradation with reliability prediction for electronic modules. *Quality and Reliability Engineering International* 2005; **21**: 715-726.
11. Huang W, Askin RG. Reliability analysis of electronic devices with multiple competing failure modes invol-

- ving performance aging degradation. *Quality and Reliability Engineering International* **19**: 241–254.
12. Crk V. Reliability assessment from degradation data. *2000 Proceedings Annual Reliability and Maintainability Symposium*, 2000; 155–161.
  13. de Oliveira RB, Colosito EA. Comparison of methods to estimate the time-to-failure distribution in degradation tests. *Quality and Reliability Engineering International* 2004; **20**: 363–373.
  14. Vázquez M, Rey-Stolle I. Photovoltaic module reliability model based on field degradation studies. *Progress in Photovoltaics: Research and Applications* 2008; **16**(5): 419–433.
  15. Terao A, Mulligan WP, Daroczi SG, Pujol OC, Verlinden PJ, Swanson RM, Miñano JC, Benítez P, Álvarez JL. A mirror-less design for micro-concentrator modules. In *IEEE 28th Photovoltaic Specialist Conference*, 2000; 1416–1419.
  16. Systems and Instruments Integration Group of IES-UPM. Private Communication.
  17. IEC 600-50-191 International Electrotechnical Vocabulary. Chapter 191: Dependability and quality of service.
  18. Meneghini M, Trevisanello L, Sanna C, Mura G, Vanzi M, Meneghesso G, Zanoni E. High temperature electro-optical degradation of InGaN/GaN HBLEDs. *Microelectronics Reliability* 2007; **47**: 1625–1629.